Gold Liquid Crystals Displaying Luminescence in the Mesophase and Short F···F Interactions in the Solid State

Rocio Bayón, Silverio Coco, and Pablo Espinet*[a]

Abstract: Rodlike gold(I) complexes, $[Au(C_6F_4OC_mH_{2m+1})(C{\equiv}NC_6H_4C_6H_4O-C_nH_{2n+1})]$ ($m=2$, $n=4$, 10; $m=6$, $n=10$; $m=10$, $n=6$, 10), display interesting features. They are liquid crystals and show photoluminescence in the mesophase, as well as in the solid state and in solution. The single-crystal, X-ray diffraction structure of $[Au(C_6F_4OC_2H_5)(C{\equiv}NC_6H_4C_6H_4OC_4H_9)]$ confirms its rodlike structure, with a linear coordination around the gold atom, and reveals the absence of any Au···Au interactions (such interactions are often present in luminescent gold complexes). Well-defined, intermolecular $F_{ortho}{\cdots}F_{meta}$ interactions, with remarkably short intermolecular F···F distances (2.66 Å), are observed; these interactions seem to be responsible for the crystal packing, which consists of an antiparallel arrangement of molecules. Experiments under different conditions support the explanation that the photoluminescence has an intramolecular origin.

Keywords: crystal engineering · fluorinated ligands · gold · isocyanide ligands · liquid crystals · luminescence

Introduction

Technologies based on luminescence require new materials integrating other physical properties. A representative case is luminescent liquid crystals, in which emission properties are combined with supramolecular organization and fluidity in the mesophase. A number of organic mesogenic derivatives have been reported to display intrinsic (that is, in the absence of other additives) luminescent properties in solution, in the microcrystalline solid state, or in thin glass films obtained by cooling the corresponding mesophase.[1] However, organic liquid crystals that display intrinsic luminescence in the mesogenic state are very scarce.[2] On the other hand, many metal complexes are strongly luminescent, but the metallomesogens reported to display photoluminescence in the solid state or in solution are just a few lanthanide derivatives and palladium complexes.[3–5] Only recently have lanthanide-based metallomesogens luminescent *in the mesophase* been reported.[6]

Gold(I) complexes frequently possess luminescence, especially in condensed phases at low temperatures; this luminescence is often attributed to the existence of Au···Au interactions.[7] Some of these complexes are halogold(I) isocyanide derivatives,[8,9] and mesomorphic gold(I) isocyanide complexes [AuX(C≡NR)] (X = anionic ligand) have also been reported.[10–12] It has been suggested (but not proven) that the formation of liquid-crystalline phases in the latter group of complexes is also helped by the presence of weak intermolecular Au···Au interactions,[10] which might be partly responsible for the higher stability of mesophases in gold mesogens, relative to other metals of the group.[13] Luminescent gold complexes containing the perfluorophenyl group are also reported to produce organometallic gold complexes with higher than average thermal stability.[14] On these grounds, we decided to synthesize and study tetrafluorophenyl gold(I) isocyanide complexes, $[Au(C_6F_4OC_mH_{2m+1})(C{\equiv}NC_6H_4C_6H_4OC_nH_{2n+1})]$, hoping that they would be mesogens, which would enable the study of the type of intermolecular interactions present in the system and the possible influence of these interactions on the complex properties. Fortunately, this family of complexes afforded examples of metallomesogens displaying good mesophase stabilization and strong photoluminescence in the mesophase, as well as in the solid state and in solution. These properties are not associated with gold–gold interactions, which are absent. Remarkably short intermolecular F···F interactions are observed for the complex studied by X-ray diffraction in the solid state.

[a] Dr. R. Bayón, Dr. S. Coco, Prof. Dr. P. Espinet
Química Inorgánica, Facultad de Ciencias
Universidad de Valladolid, 47005 Valladolid (Spain)
Fax: (+34) 983-423013
E-mail: espinet@qi.uva.es

 DOI: 10.1002/chem.200400829

Results and Discussion

Synthesis and characterization: The gold(I) isocyanide complexes were prepared according to Scheme 1[12,15] and isolated as white solids, which were fully characterized. Elemental analyses, yields, and relevant IR data of the complexes are given in the Experimental Section. All of the IR spectra are similar and show one ν(C≡N) absorption for the isocyanide group at wavenumbers about 90 cm^{-1} higher than for the corresponding free isocyanide.[12]

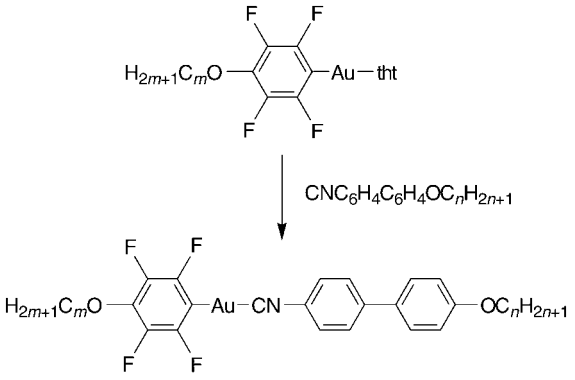

Scheme 1. Preparation of gold(I) isocyanide complexes (tht = tetrahydrothiophene).

The ^{1}H NMR (300 MHz) spectra of the gold(I) isocyanide complexes prepared are also very similar, showing four somewhat distorted "doublets" for the biphenyl group (strictly two AA′XX′ spin systems), as reported for similar gold(I) isocyanide complexes.[11,12] In addition, two triplets (quartets for the ethoxy groups) are observed at around $\delta = 4.1$ and 3.9 ppm, corresponding to the first methylene group of the $C_6F_4OC_mH_{2m+1}$ and $C_6H_4C_6H_4OC_nH_{2n+1}$ groups, respectively. The remaining chain hydrogen atoms appear in the range 0.8–1.8 ppm. The ^{19}F NMR spectra of these complexes show two somewhat distorted "doublets" flanked by two pseudotriplets, corresponding to an AA′XX′ spin system with $J_{AA'} \approx J_{XX'}$. The signals assigned to F_{ortho} and F_{meta} (reference $CFCl_3$) appear at about −118 and −157 ppm, respectively, with values of N ($N = J_{AX} + J_{AX'}$) in the range 18–19.7 Hz.

The electronic spectra of the free isocyanides and their corresponding tetrafluorophenylgold(I) isocyanide complexes are summarized in Table 1. They show two strong UV absorptions assigned to phenyl-localized π–π* transitions. The stronger absorption, assigned to a π–π* transition in the biphenyl system (K band), undergoes a noticeable bathochromic shift upon complexation of the isocyanide ligand to the gold atom. A similar effect was observed for [AuX(C≡NC$_6$H$_4$C$_6$H$_4$OC$_{10}$H$_{21}$)] (X = Cl, Br, I).[11]

Table 1. UV/Vis data for the free ligands and the complexes [Au(C$_6$F$_4$OC$_m$H$_{2m+1}$)(C$_6$H$_4$C$_6$H$_4$OC$_n$H$_{2n+1}$)].[a]

m	n	λ [nm] (ε [$dm^3 mol^{-1} cm^{-1}$])		
	4[b]	229 (11392)		288 (23119)
	6[b]	231 (8508)		283 (19950)
	10[b]	229 (7243)		289 (14870)
2[c]		230 (1043)	262 (456)	
6[c]		230 (1265)	262 (601)	
10[c]		232 (952)	262 (609)	
2	4	231 (28436)		311 (38528)
2	10	236 (11839)		305 (16191)
6	10	235 (29500)		308 (43043)
10	6	236 (20571)		310 (29160)
10	10	234 (17025)		311 (22899)

[a] In CH_2Cl_2. [b] Free isocyanide ligand. [c] $HC_6F_4OC_mH_{2m+1}$ group.

The molecular structure of [Au(C$_6$F$_4$C$_6$H$_4$OC$_2$H$_5$)(C≡NC$_6$H$_4$C$_6$H$_4$OC$_4$H$_9$)] was determined by single-crystal X-ray diffraction methods (Figure 1). The data collection and refinement parameters are detailed in the Experimental Section. The compound crystallizes in the triclinic space group $P\bar{1}$, with two formula units per unit cell. The gold atom is linearly coordinated by the isocyanide and tetrafluorophenyl groups. The bond angle C(1)-Au-C(31) is 176.4°, and the bond lengths fall within normal ranges. The dihedral angle

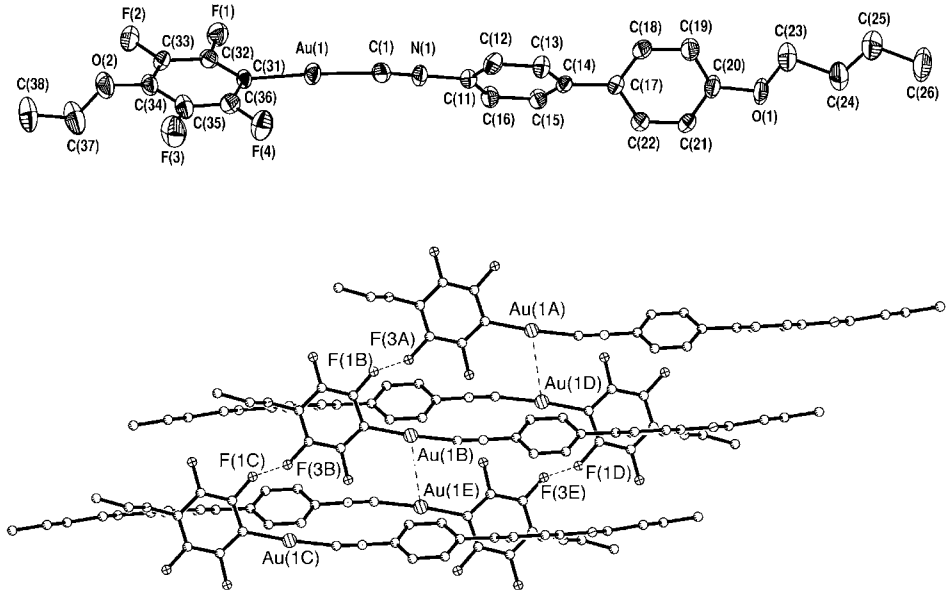

Figure 1. The crystal structure of [Au(C$_6$F$_4$C$_6$H$_4$OC$_2$H$_5$)(C≡NC$_6$H$_4$C$_6$H$_4$OC$_4$H$_9$)] (top) and a crystal-packing representation (bottom) showing some of its intermolecular features.

between the two phenyl rings of the biphenylisocyanide system is 38.2°. The butoxy chain is extended, and the molecule takes a rodlike shape. The crystal packing of the complex shows an arrangement of molecules in pairs of antiparallel corrugated layers (Figure 1 bottom and Figure 2).

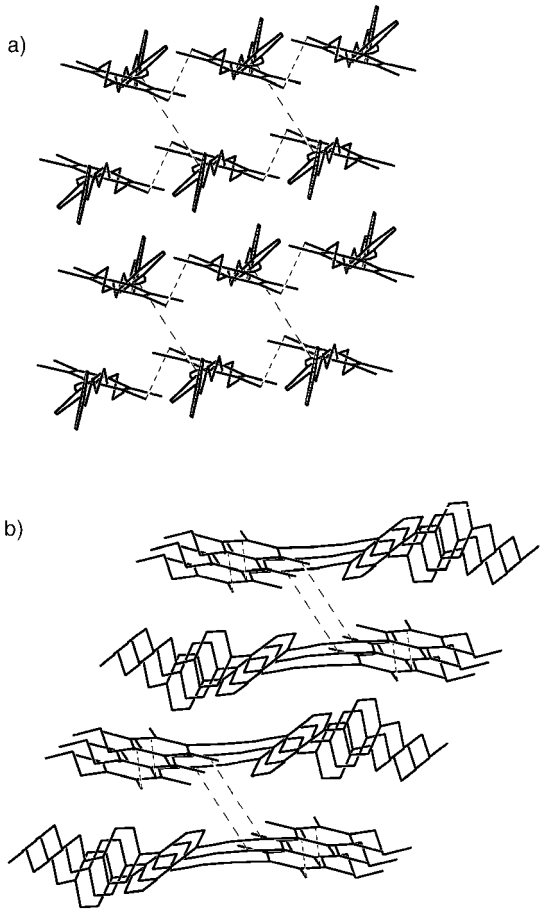

Figure 2. Two schematic views of the crystal packing in $[Au(C_6F_4C_6H_4OC_2H_5)(C{\equiv}NC_6H_4C_6H_4OC_4H_9)]$. a) View parallel to the director (long axis) of the molecules, showing the F–F contacts (short dashes), which define the corrugated layers, and the Au–Au distances (long dashes) between gold atoms in neighboring layers. b) View perpendicular to the director of the molecules again showing the F–F contacts and the Au–Au distances.

Within each layer, the molecules are parallel to each other and connected by short $F_{ortho}\cdots F_{meta}$ intermolecular distances (2.66 Å) to their neighbors. Each molecule uses one F_{ortho} and one F_{meta} atom for these connections. If we considered these connections as giving rise to a polymer, each layer could be described as a zig-zag perfluoroaryl comb "polymer", with the entire length of each gold complex hanging from the zig-zag chain and lying parallel to each other (Figure 2b). The shortest Au–Au intermolecular distance observed is 4.30 Å. This safely excludes the existence of any Au···Au interactions and corresponds to gold atoms in neighboring layers, not in the same layer.[16] Thus, the short intermolecular F···F distances are consistent with intermolecular F···F interactions and appear to be an influencing factor on the packing motif observed. Although the nature and the exact structural role of F···F interactions is not well understood yet, recent literature has provided evidence that these fluorine-based interactions, in the absence of any other significant intermolecular interactions, provide the stability to form molecular assemblies.[17,18] A search in the Cambridge Crystallographic Database for intermolecular $F_{ortho}\cdots F_{meta}$ distances below 3.0 Å in fluoroaryl metal complexes yielded 147 matches. Out of these, 26 corresponded to gold complexes, the shortest distance being 2.76 Å.[14] The influence of these fluorine-based interactions has passed unnoticed in the original literature, in which these structures were reported, but it seems to be a relevant, noncasual phenomenon to be taken into account in crystal engineering. The structure reported here possesses the shortest $F_{ortho}\cdots F_{meta}$ distance observed so far (2.66 Å), and this interaction seems to make an important contribution to the intermolecular arrangement observed in the solid.

Mesomorphic behavior: All the compounds reported here are mesomorphic. Their optical, thermal, and thermodynamic data are presented in Table 2. The increase in total chain length $(m+n)$ initially causes a decrease in the range of nematic phase as well as an increase in the range of smectic-A (SmA) phase, but for longer alkoxy chain lengths a decrease in SmA range is produced, together with an increase in smectic-C (SmC) range.

Table 2. Optical, thermal, and thermodynamic data of the complexes $[Au(C_6F_4OC_mH_{2m+1})(CNC_6H_4C_6H_4OC_nH_{2n+1})]$.

m	n	Transition[a]	Temperature[b] [°C]	ΔH[b] [kJ mol^{-1}]
2	4	C→C′	75.1	1.5
		C′→SmA	108.3	20.9
		SmA→N	177[c]	
		N→I	233.5	1.5
2	10	C→C′	65.7	1.1
		C′→SmA	81.7	30.4
		SmA→I	207.8	4.9
6	10	C→SmC	49.9	22.8
		SmC→I	209.3	5.9
10	6	C→SmC	55.4	23.5
		SmC→SmA	114[c]	
		SmA→I	205.3	5.5
10	10	C→SmC	53.4	32.2
		SmC→SmA	168.3	0.1
		SmA→I	196.3	5.8

[a] C = crystal; SmA, SmC = smectic-A, -C; I = isotropic liquid. [b] Data refers to the second DSC cycle starting from the crystal. Temperature data measured as peak onset. [c] Microscopic data.

The SmA mesophases, with their typical focal-conic fan textures on cooling from the nematic or isotropic phases, were identified by means of optical microscopy (Figure 3a). The nematic phases display the schlieren texture, showing singularities with two and four associated brushes (Figure 3b). The SmC mesophases show the typical broken

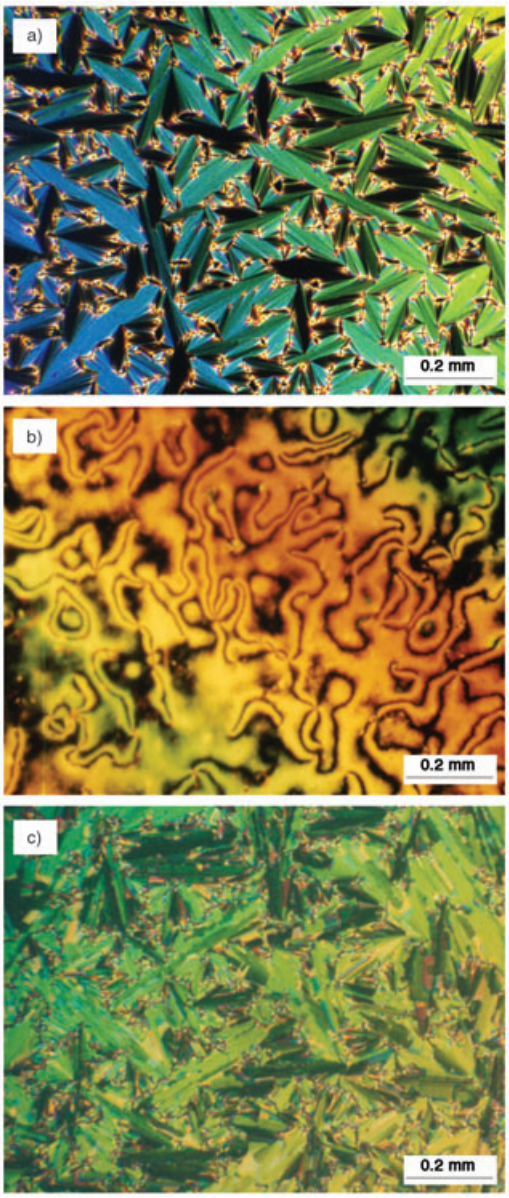

Figure 3. Polarized optical microscopic textural images (×100) observed for Au complexes. a) $[Au(C_6F_4OC_{10}H_{21})(C{\equiv}NC_6H_4CC_6H_4OC_{10}H_{21})]$: the picture shows the fan-shape texture of the SmA phase at 186 °C, on cooling from the isotropic liquid. b) $[Au(C_6F_4OC_2H_5)(C{\equiv}NC_6H_4C_6H_4OC_4H_9)]$: the picture shows the schlieren texture of the N phase at 188 °C, on cooling from the isotropic liquid. c) $[Au(C_6F_4OC_{10}H_{17})(C{\equiv}NC_6H_4C_6H_4OC_{10}H_{21})]$ at 140 °C: the picture displays the broken fan-shape texture of the SmC phase, formed on cooling from the fan-shape focal-conic area of the SmA phase.

focal-conic fan texture on cooling from the SmA phase (Figure 3c).[19–21]

Photoluminescence studies: All of the complexes are luminescent at room temperature, both in solution and in the solid state (Table 3). In the solid state they exhibit a yellow–green luminescence under UV irradiation (365 nm). All of the emission spectra are similar and consist of three broad emissions above 370 nm (for example, 384, 490, and 524 nm for $m=10$, $n=6$), whereas the free isocyanides (white solids) are luminescent and give one strong emission band with a maximum at about 360 nm. In dichloromethane, both the free isocyanides and their gold complexes are luminescent, but only one intense emission is observed for the complexes in the range 345–387 nm (Figure 4).

Table 3. Emission and excitation maxima [nm] for the free ligands and for $[Au(C_6F_4OC_mH_{2m+1})(CNC_6H_4C_6H_4OC_nH_{2n+1})]$ at 298 K.

		KBr		CH_2Cl_2	
m	n	λ_{ex}	λ_{em}	λ_{ex}	λ_{em}
	4[a]	327	354	259, 310	341
	6[a]	321	360	258, 309	355
	10[a]	282	367	282	355
2	4	358	371, 475, 506	285	345
2	10	344	375, 487, 521	274	364
6	10	348	402, 489, 523	274	363
10	6	344	384, 490, 524	276	387
10	10	343	392, 486, 520	278	362

[a] Free isocyanide ligand.

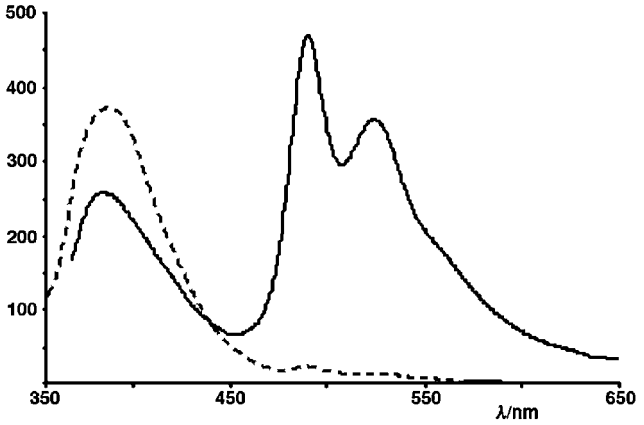

Figure 4. Emission spectra at 298 K of $[Au(C_6F_4OC_{10}H_{21})(CNC_6H_4C_6H_4OC_6H_{13})]$ ($\lambda_{exc}=344$ nm) in the solid state (solid line) and in CH_2Cl_2 (dashed line).

The lifetimes in the solid state have been measured for the complex with $m=10$ and $n=6$.[22] The emission at 384 nm has a lifetime shorter than 10 μs, the measurement limit of our spectrometer, whereas a lifetime value of 39 μs is found for both luminescence emissions at 490 and 524 nm. The lifetime values, together with the Stokes shift between the absorption and the emission bands, indicate a different nature for the last two emissions than that for the emission at 384 nm. The emission at 384 nm must be a fluorescence, involving intraligand-localized π and π* orbitals, with practically no Au contribution, as calculated for [AuClCNPh].[23] In contrast, the longer lifetimes of the emissions at 490 and 524 nm support a phosphorescence nature.

It is known that aromatic organic molecules can display relatively intense phosphorescence, arising from a triplet state that gets populated by intersystem crossing from an excited singlet state, which forms on absorption. These inter-

system crossings are helped by the presence of heavy atoms. Thus, the emissions at 490 and 524 nm would result from phosphorescent emission involving intraligand-localized states. These emissions disappear in solution, whereas that at 384 nm remains, but shifts to 387 nm. This observation can be explained by considering that, due to their long radiative lifetimes, the quenching of phosphorescent emissions is especially important in fluid media (solution), in which collisions are frequent.[22] However, as the X-ray structure of $[Au(C_6F_4C_6H_4OC_2H_5)(C{\equiv}NC_6H_4C_6H_4OC_4H_9)]$ shows intermolecular F···F interactions, the question arises whether the 490 and 524 nm emissions could be due to the molecular self-association observed in the solid, which disappears in solution? This possibility can be discarded, however, because the phosphorescent bands are recovered when diluted solutions of the complex in dichloromethane are frozen at 78 K. As, under these conditions, the F···F interactions cannot exist, the phosphorescence emissions must result mainly from intramolecular intraligand transitions.

The luminescent behavior of $[Au(C_6F_4OC_{10}H_{21})(CNC_6H_4C_6H_4OC_6H_{13})]$ is shown in Figure 5 as a function of temperature. When the sample melts to the smectic-C mesophase (at 55.4 °C), the luminescence is not lost, but its intensity decreases noticeably and continues decreasing upon further temperature increase. The emission practically disappears at about 130 °C. This process is reversible, and the intensity of the emission is gradually recovered upon cooling. Moreover, it is important to note that the bands associated with phosphorescence seem to decay with temperature more rapidly than the fluorescent emission. This behavior would be related to an increasingly efficient quenching process by collisions, as the higher temperature (and the lower viscosity) increases the molecular mobility in the mesophase. These complexes display important supercooling of the mesophase, and, as a consequence, the fluid mesophase survives at room temperature for several hours until crystallization occurs. The intensity of the emission is fully recovered at the very instant that crystallization occurs.

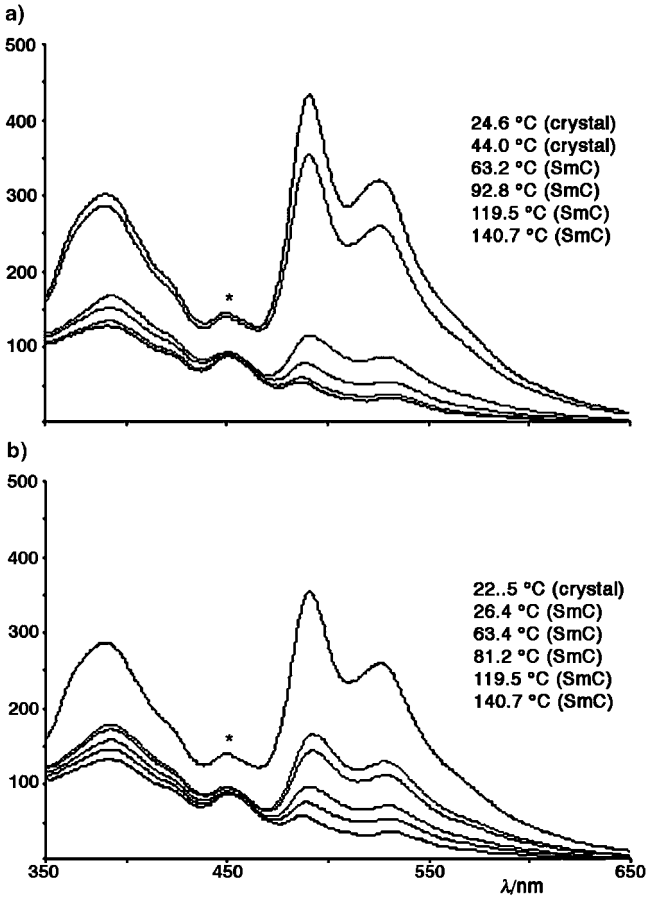

Figure 5. Emission spectra of $[Au(C_6F_4OC_{10}H_{21})(CNC_6H_4C_6H_4OC_6H_{13})]$ ($\lambda_{exc}=344$ nm) at different temperatures. The spectra and the temperature list follow the same top to bottom order. The corresponding phase is given in parenthesis. a) Heating from the crystal, and b) cooling from the SmC mesophase. Peaks marked with * are due to scattering.

Conclusions

These stable mesomorphic tetrafluorophenylgold(I) biphenylisocyanide complexes show good mesophase stabilization without gold–gold interactions in the solid state, and, consequently, probably without gold–gold interactions in the mesophase. They display remarkably short intermolecular F···F interactions (the shortest of its kind, thus far), which seem to be the driving force of the structural arrangement in the solid. Moreover, these complexes represent the first example of intrinsic luminescent metallomesogens based on organometallic complexes and display strong luminescence in the mesophase, the solid state, and in solution.

Experimental Section

Combustion analyses were carried out with a Perkin–Elmer 2400 microanalyzer. IR spectra (cm^{-1}) were recorded on a Perkin–Elmer FT 1720X instrument. ^1H and ^{19}F NMR spectra were recorded in $CDCl_3$ on Bruker AC300 or ARX300 instruments. Microscopy studies were carried out on a Leica DMRB microscope, equipped with a Mettler FP82HT hot stage (heating rate of 10 K min^{-1}) and a Mettler FP90 central processor. Differential scanning calorimetry (DSC) was carried out with a Perkin–Elmer DSC7 instrument, which was calibrated with water and indium. The scanning rate was 10 K min^{-1}, the samples were sealed in aluminum capsules in air, and the holder atmosphere was dry nitrogen. UV/Vis absorption spectra were obtained by means of a Shimadzu UV-1603 spectrophotometer, in dichloromethane ($\sim 1\times10^{-4}$ M). Luminescent data was recorded with a Perkin–Elmer LS-55 luminescence spectrometer.

Literature methods were used to prepare $HC_6F_4OC_mH_{2m+1}$,[15] $C{\equiv}NC_6H_4C_6H_4OC_nH_{2n+1}$,[11] and [AuCl(tht)] (tht = tetrahydrothiophene).[24] Only example procedures are described here, as the syntheses were similar for the rest of the compounds. Yields, IR, and analytical data are given for all the gold complexes.

Preparation of $[Au(C_6F_4OC_mH_{2m+1})(C{\equiv}NC_6H_4C_6H_4OC_nH_{2n+1})]$: A solution of *n*BuLi in hexane (0.194 mL, 0.312 mmol) was added to a solution of $HC_6F_4OC_mH_{2m+1}$ (0.312 mmol) in dried diethyl ether (25 mL) at −78 °C under nitrogen. After stirring for one hour at −50 °C, solid [AuCl(tht)] (0.96 g, 0.312 mmol) was added at −78 °C, and the reaction mixture was slowly brought to room temperature (3 h). A few drops of water were then added, and the solution was filtered in air through anhydrous $MgSO_4$. $C{\equiv}NC_6H_4C_6H_4OC_nH_{2n+1}$ (0.312 mmol) was added to the

solution obtained. After stirring for 15 min, the solvent was removed on a rotary evaporator, and the white solid obtained was recrystallized from dichloromethane/hexane at −15 °C.

***m* = 2, *n* = 4**: Yield: 56 %; IR (CH_2Cl_2): $\tilde{\nu}$ = 2214 cm^{-1} (C≡N); IR (KBr): $\tilde{\nu}$ = 2211 cm^{-1} (C≡N); elemental analysis (%) calcd for $C_{25}H_{22}AuF_4NO_2$: C 46.82, H 3.46, N 2.18; found: C 46.75, H 3.47, N 1.91.

***m* = 2, *n* = 10**: Yield: 56 %; IR (CH_2Cl_2): $\tilde{\nu}$ = 2214 cm^{-1} (C≡N); IR (KBr): $\tilde{\nu}$ = 2209 cm^{-1} (C≡N); elemental analysis (%) calcd for $C_{31}H_{34}AuF_4NO_2$: C 51.32, H 4.72, N 1.93; found: C 51.31, H 4.65, N 1.66.

***m* = 6, *n* = 10**: Yield: 34 %; IR (CH_2Cl_2): $\tilde{\nu}$ = 2214 cm^{-1} (C≡N); IR (KBr): $\tilde{\nu}$ = 2214 cm^{-1} (C≡N); elemental analysis (%) calcd for $C_{35}H_{42}AuF_4NO_2$: C 53.78, H 5.42, N 1.79; found: C 53.85, H 5.38, N 1.68.

***m* = 10, *n* = 6**: Yield: 41 %; IR (CH_2Cl_2): $\tilde{\nu}$ = 2214 cm^{-1} (C≡N); IR (KBr): $\tilde{\nu}$ = 2209 cm^{-1} (C≡N); elemental analysis (%) calcd for $C_{35}H_{42}AuF_4NO_2$: C 53.78, H 5.42, N 1.79; found: C 53.66, H 5.27, N 1.68.

***m* = 10, *n* = 10**: Yield: 40 %; IR (CH_2Cl_2): $\tilde{\nu}$ = 2214 cm^{-1} (C≡N); IR (KBr): $\tilde{\nu}$ = 2210 cm^{-1} (C≡N); elemental analysis (%) calcd for $C_{39}H_{50}AuF_4NO_2$: C 55.91, H 6.02, N 1.67; found: C 55.73, H 5.85, N 1.60.

Experimental procedure for X-ray crystallography: Crystals of [Au($C_6F_4OC_2H_5$)(C≡N$C_6H_4C_6H_4OC_4H_9$)] were obtained by direct diffusion of hexane into a solution of the complex in dichloromethane. A suitable single crystal was mounted in a glass fiber, and diffraction measurements were taken with a Bruker SMART CCD area-detector diffractometer with $Mo_{K\alpha}$ radiation (λ = 0.71073 Å).[25] Intensities were integrated from several series of exposures, each exposure covering 0.3° in ω, the total data set being a hemisphere.[26] Absorption corrections were applied based on multiple and symmetry-equivalent measurements.[27] The structure was solved by direct methods (SIR 97)[28] and refined by least-squares methods on weighted F^2 values for all reflections. Hydrogen atoms were taken into account at calculated positions, and their positional parameters were refined. Table 4 gives the data collection and refinement parameters. Refinement proceeded smoothly to give R_1 = 0.04267 on the basis of the reflections with $I > 2\sigma(I)$. Complex neutral-atom scattering factors were used.[29] CCDC-246954 contains the supplementary crystallographic data for this paper. These data can be obtained free of charge from the Cambridge Crystallographic Data Centre via www.ccdc.cam.ac.uk/data_request/cif.

Table 4. X-ray data, data collection, and refinement parameters for [Au($C_6F_4OC_2H_5$)(C≡N$C_6H_4C_6H_4OC_4H_9$)].

formula	$C_{25}H_{22}AuF_4NO_2$
M_r	641.40
crystal system	triclinic
space group	$P\bar{1}$ (no. 2)
a [Å]	7.141(3)
b [Å]	10.184(5)
c [Å]	17.713(9)
β [°]	84.715(9)
V [Å^3]	1181.7(10)
Z	2
ρ_{calcd} [g cm^{-3}]	1.803
μ [mm^{-1}]	6.278
F(000)	620
crystal size [mm]	0.25 × 0.10 × 0.05
T [K]	293(2)
θ range [°]	1.20–23.28
λ [Å]	0.71073
index ranges	$-7 \le h \le 7$
	$-11 \le k \le 10$
	$-19 \le l \le 19$
reflections collected	5277
independent reflections	3349 [R_{int} = 0.0275]
observed reflections [$I > 2\sigma(I)$]	2642
completeness to θ [°]	23.28 (98.4 %)
absorption corrections	SADABS
max/min transmission	1.000000/0.520264
data/restraints/parameters	3349/0/300
goodness-of-fit on F^2	0.986
final R indices [$I > 2\sigma(I)$]	$R1$ = 0.0427, $wR2$ = 0.0995
R indices (all data)	$R1$ = 0.0588, $wR2$ = 0.1141
largest diffraction peak/hole [e Å^{-3}]	1.712/−1.628

Acknowledgements

We are indebted to the Dirección General de Investigación (Project MAT2002-00562) and to the Junta de Castilla y León (Projects VA050/02 and VA057/03) for financial support. We thank Dr. J. M. Martín-Álvarez and Prof. D. Miguel for X-ray data acquisition, and Dr. M. Bardají for helpful discussions.

[1] a) B. P. Hoag, D. L. Gin, *Adv. Mater.* **1998**, *10*, 1546–1551; b) N. G. Pschirer, M. E. Vaughn, Y. B. Dong, H.-C. zur Loye, U. H. F. Bunz, *Chem. Commun.* **2000**, 85–86; c) A. E. A. Contoret, S. R. Farrar, S. M. Khan, M. O'Neill, G. J. Richards, M. P. Aldred, S. M. Kelly, *J. Appl. Phys.* **2003**, *93*, 1465–1467; d) F. H. Boardman, D. A. Dunmur, M. C. Grossel, G. R. Luckhurst, *Chem. Lett.* **2002**, 60–61; e) C.-H. Lee, T. Yamamoto, *Tetrahedron Lett.* **2001**, *42*, 3993–3996; f) Y. Zhang, W. Zhu, W. Wang, H. Tian, J. Su, W. Wang, *J. Mater. Chem.* **2002**, *12*, 1294–1300; g) A. J. Attias, C. Cavalli, B. Donnio, D. Guillon, P. Hapiot, J. Malthête, *Chem. Mater.* **2002**, *14*, 375–384.

[2] a) S. Kim, S. Y. Park, *Mol. Cryst. Liq. Cryst. Sci. Technol. Sect. A* **1999**, *337*, 405–408; b) A. F. Thünemann, S. Janietz, S. Anlauf, A. Wedel, *J. Mater. Chem.* **2000**, *10*, 2652–2656.

[3] For metallomesogens see: a) *Handbook of Liquid Crystals* (Eds.: D. Demus, J. Goodby, G. W. Gray, H. W. Spiess, D. V. Vill), Wiley-VCH, Weinheim, **1998**; b) *Metallomesogens* (Ed.: J. L. Serrano), VCH, Weinheim, **1996**; c) B. Donnio, D. W. Bruce, *Struct. Bonding* **1999**, *95*, 193; d) P. Espinet, *Gold Bull.* **1999**, *32*, 127–134.

[4] a) H. Nozary, C. Piguet, J.-P. Rivera, P. Tissot, P.-Y. Morgantini, J. Weber, G. Bernardinelli, J.-C. G. Bünzli, R. Deschenaux, B. Donnio, D. Guillon, *Chem. Mater.* **2002**, *14*, 1075–1090; b) K. Binnemans, L. Malykhina, V. S. Mironov, W. Haase, K. Driesen, R. Van Deun, L. Fluyt, C. Gorller-Walrand, Y. G. Galyametdinov, *ChemPhysChem* **2001**, *2*, 680–683.

[5] M. Ghedini, D. Pucci, A. Crispini, I. Aiello, F. Barigelletti, A. Gessi, O. Francescangeli, *Appl. Organomet. Chem.* **1999**, *13*, 565–581.

[6] S. Suárez, O. Mamula, D. Imbert, C. Piguet, J.-C. G. Bünzli, *Chem. Commun.* **2003**, 1226–1227.

[7] a) V. W.-W. Yam, K. K.-W. Lo, *Chem. Soc. Rev.* **1999**, *28*, 323–334; b) M. Bardají, A. Laguna, J. Vicente, P. G. Jones, *Inorg. Chem.* **2001**, *40*, 2675–2681; c) M. J. Irwin, J. J. Vittal, R. J. Puddephat, *Organometallics* **1997**, *16*, 3541–3547; d) R. L. White-Morris, M. M. Olmstead, F. Jiang, D. S. Tinti, A. L. Balch, *J. Am. Chem. Soc.* **2002**, *124*, 2327–2336; e) Y.-A. Lee, J. E. McGarrah, R. J. Lachicotte, R. Eisenberg, *J. Am. Chem. Soc.* **2002**, *124*, 10662–10663; f) J. P. Fackler, Jr., *Inorg. Chem.* **2002**, *41*, 6959–6972.

[8] R. L. White-Morris, M. Stender, D. S. Tinti, A. L. Balch, D. Rios, S. Attar, *Inorg. Chem.* **2003**, *42*, 3237–3244.

[9] H. Ecken, M. M. Olmsted, B. C. Noll, S. Attar, B. Schlyer, A. L. Balch, *J. Chem. Soc. Dalton Trans.* **1998**, 3715–3720.

[10] T. Kaharu, R. Ishii, S. Takahashi, *J. Chem. Soc. Chem. Commun.* **1994**, 1349–1350.

[11] M. Benouazzane, S. Coco, P. Espinet, J. M. Martín-Álvarez, *J. Mater. Chem.* **1995**, *5*, 441–445.

[12] R. Bayón, S. Coco, P. Espinet, *Chem. Mater.* **2002**, *14*, 3515–3518.

[13] M. Benouazzane, S. Coco, P. Espinet, J. Barberá, *J. Mater. Chem.* **2001**, *11*, 1740–1744.

[14] E. J. Fernández, P. G. Jones, A. Laguna, J. M. López-de-Luzuriaga, M. Monge, J. Pérez, M. E. Olmos, *Inorg. Chem.* **2002**, *41*, 1056–1063.

[15] S. Coco, C. Fernández-Mayordomo, S. Falagán, P. Espinet, *Inorg. Chim. Acta* **2003**, *350*, 366–370.
[16] W. Schneider, K. Angermaier, A. Sladek, H. Schmidbaur, *Z. Naturforsch.* **1996**, *51b*, 790–800.
[17] A. R. Choudhury, T. G. Row, *Cryst. Growth Des.* **2004**, *4*, 47–52.
[18] A. R. Choudhury, U. K. Urs, T. N. Guru Row, K. Nagarajan, *J. Mol. Struct.* **2002**, *605*, 71–77.
[19] D. Demus, L. Richter in *Textures of Liquid Crystals*, 2nd ed., VEB Deutscher Verlag für Grundstoffindustrie, Leipzig, **1980**.
[20] G. W. Gray, J. Goodby in *Smectic Liquid Crystals. Textures and Structures*, Leonard Hill, Glasgow and London, **1984**.
[21] I. Dierking in *Textures of Liquid Crystals*, Wiley-VCH, Weinheim, **2003**.
[22] C. E. Wayne, R. P. Wayne in *Photochemistry*, Oxford University Press, New York, **1996**.
[23] J. Gagnon, M. Drouin, P. D. Harvey, *Inorg. Chem.* **2001**, *40*, 6052–6056.
[24] R. Usón, A. Laguna, J. Vicente, *J. Organomet. Chem.* **1977**, *131*, 471–475.
[25] SMART V5.051 Diffractometer Control Software, Bruker Analytical X-ray Instruments, Madison, WI, **1998**.
[26] SAINT V6.02 Integration Software, Bruker Analytical X-ray Instruments, Madison, WI, **1999**.
[27] G. M. Sheldrick, SADABS: A program for absorption correction with the Siemens SMART system, University of Göttingen, Göttingen (Germany), **1996**.
[28] A. Altomare, M. C. Burla, M. Camalli, G. L. Cascarano, C. Giacovazzo, A. Guagliardi, A. G. G. Moliterni, G. Polidori, R. Spagna, *J. Appl. Crystallogr.* **1999**, *32*, 115–119.
[29] *International Tables for Crystallography, Vol. C*, Kluwer, Dordrecht, **1992**.

Received: August 11, 2004
Published online: December 22, 2004

